



Adaptive sliding window segmentation for physical activity recognition using a single tri-axial accelerometer



Mohd Halim Mohd Noor^{a,b,*}, Zoran Salcic^a, Kevin I-Kai Wang^a

^a The University of Auckland, Auckland, New Zealand

^b Faculty of Electrical Engineering, Universiti Teknologi MARA, Penang, Malaysia

ARTICLE INFO

Article history:

Received 11 March 2016

Received in revised form 14 September 2016

Accepted 15 September 2016

Available online 23 September 2016

Keywords:

Activity recognition

Activity transition diagram

Adaptive sliding window

Signal segmentation

ABSTRACT

Previous studies on physical activity recognition have utilized various fixed window sizes for signal segmentation targeting specific activities. Naturally, an optimum window size varies depending on the characteristics of activity signals and fixed window size will not produce good segmentation for all activities. This paper presents a novel approach to activity signal segmentation for physical activity recognition. Central to the approach is that the window size is adaptively adjusted according to the probability of the signal belongs to a particular activity to achieve the most effective segmentation. In addition, an activity transition diagram for activity recognition is developed to validate the activity transition and improve recognition accuracy. The adaptive sliding window segmentation algorithm and the role of activity transition diagram are described in the context of physical activity recognition. The approach recognizes not only well defined static and dynamic activities, but also transitional activities. The presented approach has been implemented, evaluated and compared with an existing state-of-the-art approach by using internal and public datasets which contains activity signals of dynamic, static and transitional activities. Results have shown that the proposed adaptive sliding window segmentation achieves overall accuracy of 95.4% in all activities considered in the experiments compared to the existing approach which achieved an overall accuracy of 89.9%. The proposed approach achieved an overall accuracy of 96.5% compared to 91.9% overall accuracy with the existing approach when tested on the public dataset.

© 2016 Elsevier B.V. All rights reserved.

1. Introduction

Aging and dependent population is recognized as a major social and economic issue for the coming decades. According to World Health Organization, it is estimated that there will be 2 billion people of age 60 and older by 2050 [1]. In Europe, it is expected that the elderly population of European Union (EU27) aged 65 years or over to rise to 30% in 2060 [2]. Elders who are dependent and vulnerable in different aspects due to cognitive and physical impairment require assistance in their activities of daily living (ADL). With the increase of elderly population, rise in health care cost with insufficient and ineffective care is becoming an issue in the future. One of the promising solutions to mitigate the issue is known as assisted living systems [3]. The aim of such system is to allow elders to live independently at home and at the same time enhance their living quality. As a result, the cost for society and public health system could be reduced [4].

* Corresponding author at: The University of Auckland, Auckland, New Zealand.

E-mail addresses: mmoh626@aucklanduni.ac.nz, mohalimnoor@gmail.com (M.H.M. Noor).

Assisted living system incorporates sensing, actuation and networking technologies and data processing techniques to provide assistance to elderly people with their daily activities and help them to be safe and healthy while living independently. One of the main components of assisted living system is human activity recognition (HAR) [3]. HAR is a system that provides information about people's actions and behavior. The system commonly uses ambient and wearable sensors for gathering signals and processes them through machine learning techniques for classification. The activity information can be used by the assisted living system to react and adapt to the circumstance of the user, allowing preventive measures to be taken if necessary. For example, the stove can be automatically switched off if it is on without being attended to for a long time. The information can also be used by health care professionals, caregivers and their families to provide information and intelligent services. In context-aware elderly care system, physical activity is an essential context for higher level context information to be inferred such as ADL and situation [5,6].

Transitional activities such as rising from a chair and sitting down is a prerequisite for maintaining independent living. Difficulties in performing these activities can limit independence and lead to a less active lifestyle and a subsequent deterioration in health [7–9]. Falls cause two thirds of fatal death in elderly people aged 65 years or older [10], and they are the most common type of accidents among the elders [11]. Most falls occurred during postural transition activities such as from standing to sitting and vice versa and when initiating walking [12,13]. Several features of sit-to-stand or stand-to-sit performance have been associated with falls or fall risks such as transition duration and number of successful attempts [11,14]. Therefore, it is important to recognize transitional activities so that early preventive measures can be provided to prevent fall incidents.

Activity recognition usually segments the sensor signals into windows for the successive features extraction and classification. The size of the segmented windows is empirically selected based on past experiments and hardware limitations for specific types of activity recognition. Majority of approaches used window size in the range of 1–6.7 s while a few of them used larger window size such as 10 and 12.8 s [15–18]. As a result, the developed techniques may not be applicable to be trained for recognizing different activities. In addition, misclassifications could still happen especially for transitional activities. This is due to the fact that the length of transitional activity signals varies depending on the time to complete the activity [17,18]. Evidently, a sliding window with a fixed size is not an effective approach for activity recognition system. This is the motivation for our proposed approach in which the window size is dynamically adapted during classification, based on certain characteristics in the signal, to better capture signals of different activities.

The main objective of this work is to develop a systematic adaptive signal segmentation approach for physical activity recognition based on the use of a single accelerometer. In this paper, the foundation of adaptive sliding window approach is presented. The approach can detect not only static and dynamic, but also transitional activity signals of varying period as the segmentation window is being evaluated and its size adapted dynamically. The window size is adaptively adjusted based on the continuous evaluation of the activity signals. As a result, a more effective window size can be selected for segmentation to achieve more accurate classification. In addition, the transition model of physical activity in the form of a transition diagram is proposed and integrated with the activity classification algorithm resulting in higher recognition accuracy.

The rest of the paper is organized as follows. Some currently used signal segmentation techniques and physical activity recognition systems relevant for this work are presented in Section 2 followed by the characterization of activity signals and the rationale behind the introduction of adaptive sliding window in Section 3. Adaptive sliding window segmentation algorithm and the role of activity transition diagram (ATD) in enhancing physical activity recognition are described in Section 4. Then, data collection, features selection, classifiers construction and experimental setup for activity recognition are described in Section 5. Section 6 presents the results, as well as their comparison with the existing state-of-the-art approach. Finally, Section 7 contains the conclusions.

2. Related works

2.1. Existing signal segmentation approaches

In vision-based activity recognition, video segmentation is used to obtain a segmented video of a single action. One of the common action segmentation techniques is boundary detection where boundaries are defined as discontinuities in acceleration of the observed motions. A sliding window is a technique where video sequence is divided into overlapping segments and classification is performed on all the segments to define the action segmentation. Another technique for action segmentation is to model the transitions between actions by concatenating action grammars [19]. In sensor-based activity recognition, signal segmentation is a technique of dividing a large signal into smaller segments for processing and has direct impact on the quality of feature extraction and classification accuracy [20]. At the same time, it also determines suitability of the approach for real-time operation. Numerous techniques have been proposed for signal segmentation. Santos et al. [21] proposed an adaptive sliding window approach to improve segmentation of human action sequences for activity recognition. In the approach, window size and time shift are dynamically adjusted based on entropy feedback to improve the classification results. However, the experiments do not involve transitions between activities such as stand-to-sit, sit-to-lie and lie-to-sit. Furthermore, the algorithm could be computationally expensive since shorter time shifts would increase the rate of classifications per second. Kozina and Lustrek [22] proposed a segmentation algorithm that searches for significant differences between consecutive samples which is defined by the reduction of the samples' values exceed certain

threshold. The threshold is determined by the difference of average maximum and minimum values of a set of samples. Bifet & Gavaldà [23] proposed a segmentation algorithm that can adapt the window size according to the determination of concept drift (change in data stream) in which, the window size is increased when the data values in the window are stable (low concept drift) to include more training instances and decrease otherwise. The change detection is based on mean difference of two sub-windows is greater than a given threshold. However, the algorithms are sensitive to noise such as abnormal high or low peaks which is very common in acceleration data. Núñez et al. [24] proposed the OnlineTree2 algorithm which uses an adaptive windowing technique to induce improved decision tree by evaluating the performance of the decision tree. Sheng et al. [25] proposed an adaptive time window method to extract features from quasi-periodic signals more accurately for activity recognition. The method uses pitch extraction algorithms to achieve more effective segmentation. The experiments involve dynamic and static activities only. Activity-defined techniques detect changes in activity and take the initial and end time as segmentation boundaries. Then, the specific activity in the window is identified. In [26,27], wavelet analysis is used to detect changes in frequency characteristics which indicate changes in activity. In [28], changing point which is defined by the change in action from static activity to dynamic activity and vice versa is detected by calculating the displacement of sensor data, and from this point the window segmentation is set and classified. Event-defined techniques locate specific events such as heel strikes and toe-offs to segment a signal [29,30]. The detection of events is achieved by filtering the signals to produce resultant signals which indicate the location of the events. In [31], wavelet analysis is used to detect the heel strikes and toe-offs events. Jasiewicz et al. [32] uses foot linear accelerations and foot sagittal angular velocity to detect the events. Benocci et al. [33] detects walking tasks on loaded conditions by identifying gait cycle through heel strike events. Symbol-based method is used to detect heel strikes and toe-offs events in [34]. Sliding window is the most widely used technique in activity recognition due to its simplicity. It segments the signal into a window of fixed size for features extraction and classification. Then the window is shifted to segment new sensor data with a degree of overlap. A degree of 50% would shift the window by half of its size, which means 50% of the previous data are included in the window. A degree of 0% means that the windows are not overlapping. Various window sizes from 0.1 to 12.8 s have been used in previous studies [15–18]. However, in our study we have found that fixed sliding window is not an effective segmentation approach for activity recognition because the lengths of transitional activities are varies from one to another. A small window size could split an activity signal while large window size could contain multiple activity signals. Both cases could lead to suboptimal information for an activity classification algorithm.

2.2. Physical activity recognition system

Numerous HAR systems have been proposed for elderly care applications. Numerous sensors have been studied to determine their effectiveness in activity recognition application and inertial sensors, specifically accelerometers are the most frequently used and found to be effective in monitoring physical activities such as walking, running, standing and sitting [35]. Most of the studies investigated the use of either multiple accelerometers worn on different body parts [36–39] or a single accelerometer worn on a specific part of a body. Some of the studies utilized accelerometers with other sensors such as barometer, electrocardiogram (ECG) and GPS [40,41]. Multiple attachment of sensors allows the systems to recognize complex activities such as cooking, grooming and cleaning with high accuracy. However, these systems are not feasible for long-term activity monitoring because they impede subject's daily physical activities due to multiple attachments to the body [42]. The use of single accelerometer has been investigated for activity recognition with encouraging results [40,41, 43–47]. The focus of the studies is to recognize physical activities such as ambulation activities (walking, running), body postures (sitting, standing) and postural transitions. In [40,41,43–45], fixed window size in the range of 2.56 and 10 s are used to classify the activity signals. In [46,47], wavelet transform is used to decompose the raw acceleration signals to extract wavelet features such as low-frequency components and wavelet coefficients using 2.56 and 10.24 s window with 50% overlapping. The results show wavelet transform can discriminate the activities effectively. However, according to [48], time-frequency features outperforms the wavelet features in the performed experiments. All the aforementioned works do not consider transitional activities in their studies.

Transitional activities are usually disregarded in activity recognition since the number and length of transition windows is relatively lower and shorter than other activities as reported in [49]. A number of systems have been proposed which consider transitional activities in the classification. Kozina et al. [50] proposed a new architecture for activity recognition to recognize ADL, exercise activities and seven transitional activities using three accelerometers. The architecture consists of three layers, in which knowledge-based and machine learning classifiers are implemented in the first two layers. The outputs of the classifiers are aggregated and fed to the top layer to correct the final decision of the recognized activity using a Hidden Markov Model. In [51], an algorithm is designed to compute tilting angles using signals from three wearable sensors. The computed tilt angles are used to classify walking, body postures and postural transitions such as stand-to-sit and sit-to-stand. However these systems require multiple attachment of sensors to the body. Ahanathapillai et al. [52] utilized a single accelerometer worn on the wrist to recognize walking, sitting, stand-to-sit and sit-to-stand. Using k-NN, accuracy rate of 89% was achieved. Window size is not mentioned in the study. Khan et al. [53] utilized a single accelerometer to recognize physical activities including postural transitions such as stand-to-sit, sit-to-lie and stand-to-walk with accuracy of 97.9%. However, fixed window size of 3.2 s is used which can give rise to an increase in false negative rate especially when the main focus is ambulation activities and body postures rather than transitions.

Table 1

Comparison of different related works that dealing with transitional activities.

Referenced work	Wearable sensing component	Activities recognized
Reyes-Ortiz and colleagues	Single wearable sensor: accelerometer and gyroscope.	Seven activities: walking, walking upstairs, walking downstairs, standing, sitting, lying down and postural transition.
Gupta and Dallas	Sing wearable sensor: accelerometer.	Six activities: walking, running, jumping, staying stationary, sit-to-stand/stand-to-sit and stand-to-kneel-to-stand.
Adaptive sliding window (this article)	Single wearable sensor: accelerometer.	Ten activities: walking, standing, sitting, lying face-up, lying face-down, stand-to-sit, sit-to-stand, sit-to-lie, lie-to-sit, falling.

Reyes-Ortiz et al. [54] presented the Transition-Aware Human Activity Recognition to deal with transitional activities: stand-to-sit, sit-to-stand, sit-to-lie, lie-to-sit, stand-to-lie and lie-to-stand. 2.56 s and 50% fixed window overlap is used to classify the signals from an accelerometer and a gyroscope attached to the waist. The approach uses heuristic filtering technique to filter a sequence of classification in the form of probability vectors to recognize transitional activities by measuring the length of the signal activation. A transitional activity is determined if the signal activation does not exceed a threshold. However, the system does not distinguish between the different transitional activities in which the transitional activities are classified as postural transition. The proposed approach achieved overall accuracy of 96.7%. Gupta and Dallas [55] introduced new features to effectively capture the characteristics of transitional activities: stand-to-sit/sit-to-stand and stand-to-kneel-to-stand. The features are mean trend, windowed mean difference, variance trend, windowed variance difference. These features further break the fixed window size of 6 s which was used in the study into 0.5 s sub-windows with no overlap, and extract the characteristics of the signals within the sub-windows. They also evaluated features called detrended fluctuation analysis coefficient, uncorrelated energy and maximum difference acceleration to capture the correlation and uncorrelation between signals. The features were chosen ahead of other features such as mean, variance and energy by Relief-Feature (Relief-F) selection algorithm and wrapper-based sequential forward floating search (SFFS). The proposed approach achieved overall accuracy of 98%. However, stand-to-sit and sit-to-stand are not distinguished by the system in which the activities are classified as a single class (sit-to-stand/stand-to-sit). Table 1 shows the comparison of the related works and our proposed approach in terms of wearable sensing component and activities recognized.

All presented existing approaches used sliding window technique with various fixed window sizes and degrees of overlapping without discussing criteria for selecting window size. The impact of window size on the performance of activity recognition system has been investigated in [17,18]. The results show a variation in accuracy between the different window sizes, with transitions being most often misclassified. In this work, the transitional activities are targeted by adaptively adjusts the size of segmentation based on the signal information. Therefore, a more effective segmentation can be selected to achieve more accurate classification. We validate the proposed algorithm with an internal and public datasets. The datasets contain physical activities and transitional activity signals of different lengths which is required for the evaluation of the system. Additionally, we have implemented the state-of-the-art approach described in [55] to compare with the proposed approach. This work is, to the best of our knowledge, the first to propose an adaptive sliding window to deal with transitional activities.

3. Characterization of activity signals

A key factor in signal segmentation is to select the suitable window size for activity classification. Window size is important because it needs to capture necessary characteristics of a signal in order to achieve correct detection/classification. Short windows could slice an activity signal into multiple separate windows. Thus a truncated signal lacks the full information to describe the activity. On the other hand, larger window size could contain multiple activity signals which could also lead to misinterpretation of physical activities. The most effective window size depends on the type of signals being evaluated because different activities have different periods of motion. The scenario is shown in Fig. 1. The signal contains three activity signals (A1, A2 and A3) with varying length. The fixed sliding window with 50% overlapping is employed to classify the activities. As shown in Fig. 1, only signal A2 is shorter than the window size while signals A1 and A3 are longer. Therefore, the signals are not fully segmented by window W1, W2 and W4. In both cases, misclassification could happen because the windows do not have optimal information of the signals.

To demonstrate the differences in signal characteristics and motion periods, three scenarios of activity signal are considered and illustrated in Figs. 2 and 3. The signals are generated at 50 Hz by an accelerometer attached to the right waist. In the first scenario, the signals are generated by dynamic activity. Dynamic activity signal exhibits periodic behavior with high frequency components and the trend is generally flat. An acceleration signal along the horizontal axis, A_y of a dynamic activity (walking) is illustrated in Fig. 2(a). The second scenario involves segmenting signals generated by static activities. Since static activities do not involve much body movement, the generated signals have almost constant magnitude values and very low frequency components. Therefore, the trend of the signals is also generally flat. Fig. 2(b) illustrates the acceleration signal along the horizontal axis, A_y of the standing activity.

In the third scenario, the signals have low frequency components and the magnitude is either increasing or decreasing. Furthermore, the signal length is varying from one to another. This type of signal is generated by transitional activities. For example, from the position of standing to sitting, the trend of the acceleration signal along the horizontal axis is decreasing

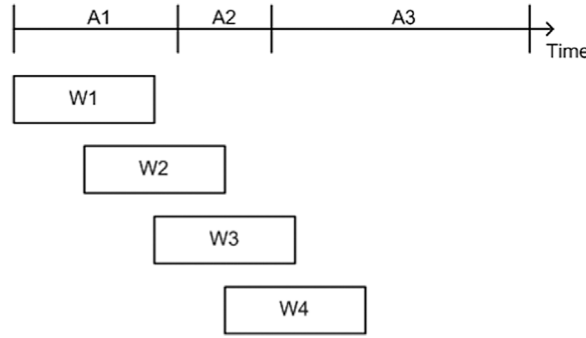


Fig. 1. Activity classification with fixed sliding window.

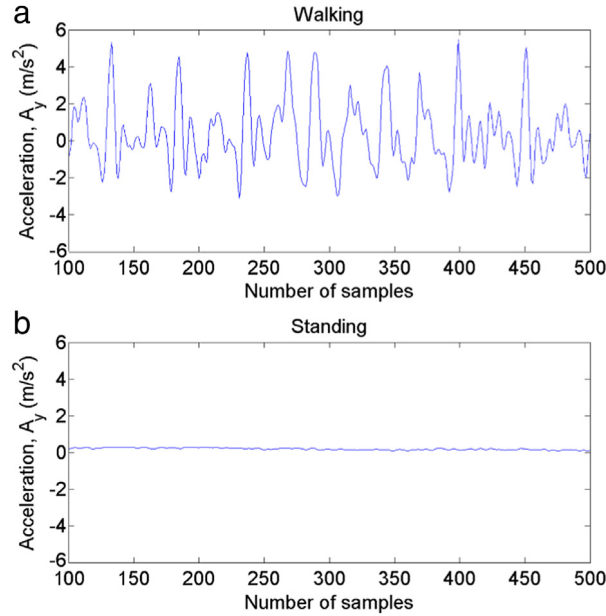


Fig. 2. Acceleration plots for (a) walking activity and (b) standing activity.

before the magnitude is stabilized at -5 m/s^2 , and it takes 2.5 s (125 samples) to complete as illustrated in Fig. 3(a). The flat signal indicates the person is in sitting position. Conversely, when the person is getting up, the trend of the signal is increasing before the magnitude stabilizes at 0 m/s^2 , and it takes 0.4 s (20 samples) longer to complete as shown in Fig. 3(b). Evidently, fixed size window is not the most effective approach to achieve accurate activity recognition due to the diverse characteristics and periods of different activity signals.

In this paper, we present the adaptive sliding window algorithm for physical activity recognition as shown in Fig. 4. In Fig. 4, activity signals of varying length are being classified by employing adaptive sliding window. The algorithm has an initial size of window used for segmentation which can be expanded dynamically to accommodate more samples if the signal is deemed longer than the current window size. The scenario is shown in Fig. 4, in which windows W1' and W3' are the actual segmentation window expanded from W1 and W3 respectively since signals A1 and A3 are longer than initial window size. In this way, a more effective segmentation for classification can be achieved. The key challenges are the criteria for triggering window size expansion, how to adapt the window size to capture the whole signal and how to determine the most effective window size.

4. Proposed method

The block diagram of the proposed physical activity recognition system is given in Fig. 5. The activity signal from accelerometer is pre-processed for noise filtering. Then, relevant features are extracted from the signal for activity classification. The classification system consists of three classifiers: transitional activity detector, non-transitional activity classifier and transitional activity classifier. All three classifiers are implemented as a Decision Tree. The implementation of the classifiers is described in Section 5.2. The function of transitional activity detector is to differentiate transitional activity

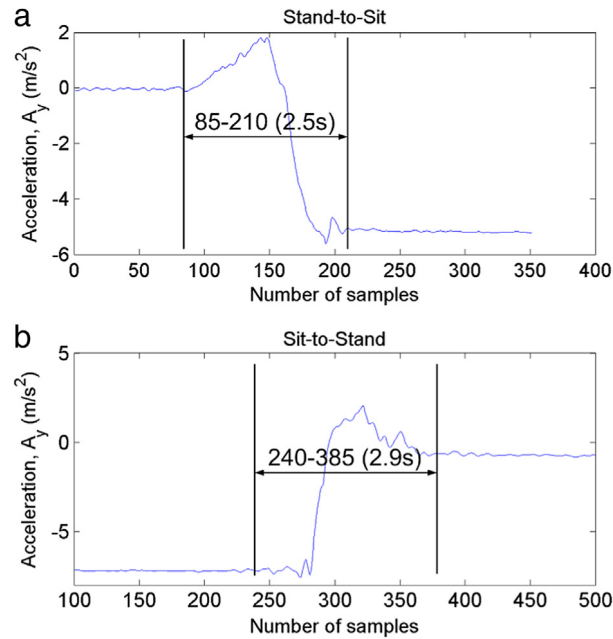


Fig. 3. Acceleration plots for stand-to-sit activity and sit-to-stand activity signals sampled at a rate of 50 Hz.

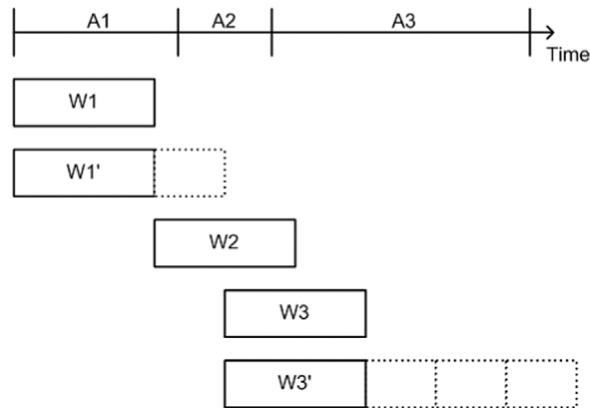


Fig. 4. Activity classification with adaptive sliding window.

signal from static/dynamic activity signals by processing the signal in the fixed initial window size. When transitional activity signal is identified, adaptive sliding window is executed and the signal is classified by transitional activity classifier. Then, the window is expanded to determine the most effective segmentation by calculating the probability of the segmented signal belong to a particular activity given a set of features, which is classified by transitional activity classifier. Multivariate Gaussian distribution is used to calculate the probability. The window will be expanded as long as the calculated probability is increasing in each iteration. If the signal is non-transitional activity, fixed sliding window is executed and the signal is classified by non-transitional activity classifier.

In order to make a classification of an activity more robust, a further enhancement of activity recognition is proposed by integration of a transition model of physical activities represented by an ATD, in the activity recognition system. The ATD is a part of the state validator of the activity recognition system. The role of the state validator is to provide feedbacks to the system in order to improve the accuracy of classification. The state validator consists of invalid activity transition detector, three state buffers and ATD. The function of invalid activity transition detector is to check the validity of an activity transition. State buffers are to store the three consecutively classified activities, the current one and two immediately preceding ones. The classification system provides the recognized activity for every classified window to the state validator. Each time the current activity is updated, the activity transition validity is checked by the invalid activity transition detector. In the case of an invalid activity transition, multivariate Gaussian distribution is applied to re-classify the signal. Next possible activities are acquired from ATD to aid the re-classification process.

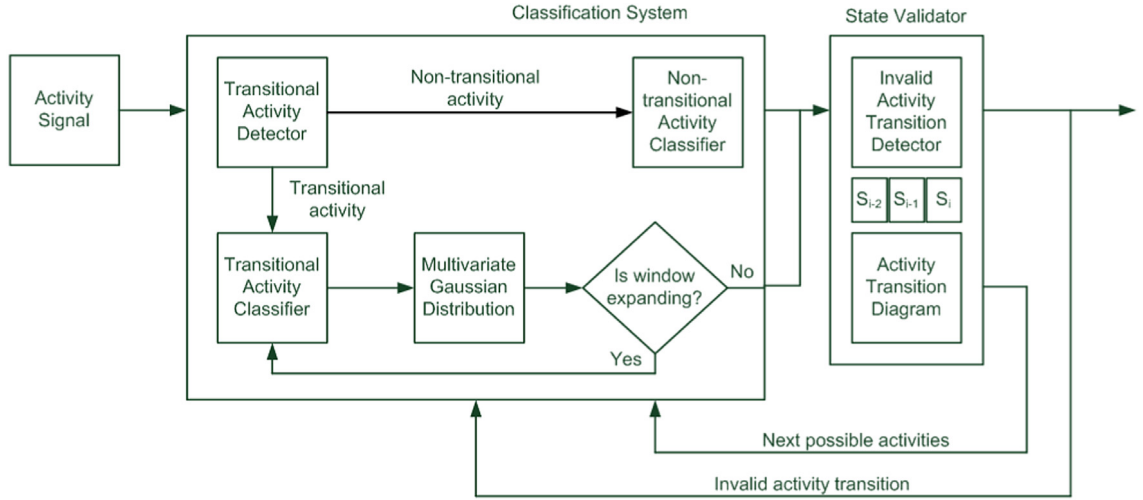


Fig. 5. The block diagram of physical activity recognition system.

4.1. Adaptive sliding window

The proposed algorithm requires transitional activity signals to be detected in order to trigger the usage of adaptive sliding window technique. Therefore, a feature that can effectively capture the acceleration trend (increasing or decreasing) needs to be determined for identifying the transitional activity. The process of selecting the features for transitional activity detector is described in Section 5.2. The pseudo-code is shown in Fig. 6. The algorithm starts with an initial (default) window size for signal segmentation and classification. The algorithm first distinguishes non-transitional activity (static/dynamic activity) and transitional activity as the windows are being evaluated as defined by line 1–2. Detection of transitional activity signal is performed for every window classification. If a transitional activity window is detected, adaptive sliding window algorithm is executed to expand the window size and segment the transitional activity signal. Otherwise, the window will be classified by the non-transitional (dynamic/static) activity classifier as defined by lines 4. Lines 6–16 define the adaptive sliding window process, which are executed whenever transitional activity signal is detected. The algorithm starts with extracting features to be evaluated by transitional activity classifier, and then calculates the probability density function (PDF) of the classified activity which is used to determine the most effective window segmentation.

Probability density function of d -dimensional data (features) $x = \{x\}$ given an activity, A_j , denoted by $p(x; \mu_j, \Sigma_j)$ is calculated by using multivariate Gaussian distribution, which allows correlation between multiple features and their relevance to the problem to be modeled [56] as follows. Probability density function is the likelihood that a signal belongs to a particular activity, which is used to determine the most effective window segmentation.

$$p(x|A_j) \propto p(x; \mu_j, \Sigma_j) = \frac{1}{(2\pi)^{n/2} |\Sigma_j|^{1/2}} e^{-\frac{1}{2}(x-\mu_j)^T \Sigma_j^{-1}(x-\mu_j)} \quad (1)$$

where n is the dimension of the feature vector. μ_j is the mean matrix and Σ_j is the covariance matrix corresponding to the features extracted from the window. Parameters μ_j and Σ_j are estimated from the training datasets as follows:

$$\mu_j = \frac{1}{N_j} \sum_{x \in A_j} x \quad (2)$$

$$\Sigma_j = \frac{1}{N_j} \sum_{x \in A_j} xx^T - \mu_j \mu_j^T \quad (3)$$

where N_j is the total number of observations belonging to activity, A_j . The same features used by the regular classifiers are used to model the distribution.

Based on the recognition result and PDF, the window may be expanded to capture a longer duration transitional activity signal. Window expansion algorithm is an iterative process in which the window size is expanded by an expansion factor (ef) of the initial window size as defined by line 12. The expansion factor in the range of $0 \leq ef \leq 1$ is predefined to determine the size of window expansion. A value of one ($ef = 1$) indicates that the window is expanded by the size of the initial window. In each iteration, the features of the signal are computed for the transitional activity classifier to be evaluated. Then the PDF of the window corresponding to the activity is calculated. The window will continue expanding until the most effective window segmentation is found. The most effective window segmentation is the window with the highest probability density function value.

w is the size of initial window in number of samples.

of is the window overlapping factor in the range of $0 \leq of \leq 1$.

ef is the window expansion factor in the range of $0 \leq ef \leq 1$.

k is the number of window expansions, where $k = 0, 1, \dots, k_{max}$ and k_{max} is the maximum number of allowed window expansion.

$N_{i,k}$ is the number of samples in window i after k expansion, where $N_{i,0} = w$.

$S_{i,j}$ is a sample in window i , where $j = 0, 1, 2, \dots, N_{i,k} - 1$ is the sample index within the window.

$p_{S_{i,j,k}}(\mathbf{x}|A)$ is the probability density function of extracted features, \mathbf{x} , from samples of window i after k expansion given an activity A .

p_{max} is the maximum probability density function value for a window expansion to determine the most effective window segmentation.

$round(i)$ is rounding i to the nearest integer.

1. calculate features of the signal
2. execute transitional activity detector
- 3: **if** non-transitional activity **then**
- 4: activity, $A =$ execute non-transitional (dynamic/static) activity classifier
- 5: **else**
- 6: **while** $k \leq k_{max}$ **do**
- 7: calculate features of the signal
- 8: activity, $A =$ execute transitional activity classifier
- 9: calculate probability density function, $p_{S_{i,j,k}}(\mathbf{x}|A)$
- 10: **if** A is not changed or $p_{S_{i,j,k}} > p_{max}$ **then**
- 11: $p_{max} = p_{S_{i,j,k}}$
- 12: $N_{i,k} = w + round(ef \times w) \times k$
- 13: **else**
- 14: stop window expansion
- 15: **end if**
- 16: **end while**
- 17: **end if**
- 18: $S_{i+1,0} = S_{i,v}$ where $v = (N_{i,k} - 1) - round(of \times w)$

Fig. 6. Adaptive sliding window algorithm.

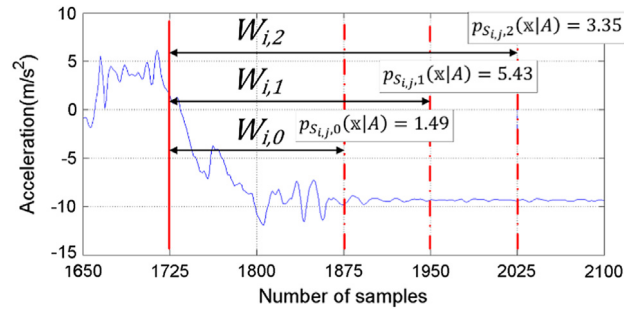


Fig. 7. Window expansion scenario.

One window expansion scenario is illustrated in Fig. 7. Fig. 7 shows that the window has been expanded two times. $W_{i,0}$, $W_{i,1}$ and $W_{i,2}$ denote the initial window and the windows after each expansion. The PDF for each window is denoted by $p_{S_{i,j,0}}$, $p_{S_{i,j,1}}$ and $p_{S_{i,j,2}}$. In this scenario, since PDF value of $W_{i,2}$ is lower than the PDF value of $W_{i,1}$, the window expansion operation is stopped at $W_{i,2}$ and $W_{i,1}$ is determined as the most effective window segmentation.

Three conditions are defined as stopping conditions of the window expansion. Firstly, classification of current iteration is found to be different than the initial classification. Initial classification is defined by the transitional activity classifier in the first iteration of window expansion. If classification result is changed in the next iteration, it is assumed the window contains other activity signal and hence affecting the classification. Secondly, the computed probability density function of current iteration is lower than of the previous iteration. This indicates the window contains other activity signal which is the reason of the smaller PDF value. Lastly, the window reaches its maximum number of expansions and the window stop expanding. After window classification process is finished, line 18 shifts the window forward to segment new samples with an overlapping factor (of). The overlapping factor determines the number of samples from current window to be overlapped by the next window. In other words, the new window will contain some samples from the previous window. The overlapping factor is in the range of $0 \leq of \leq 1$.

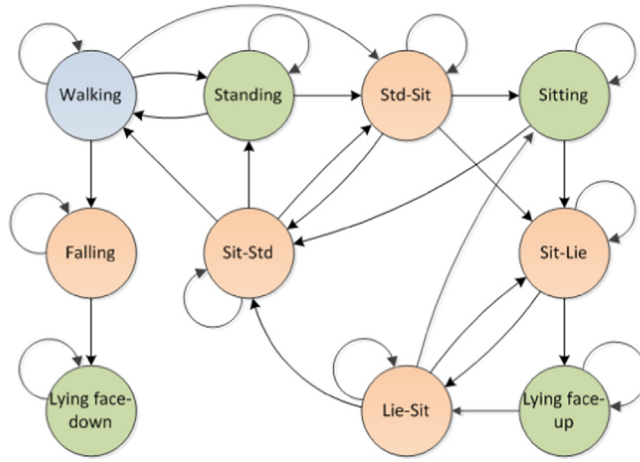


Fig. 8. Activity transition diagram.

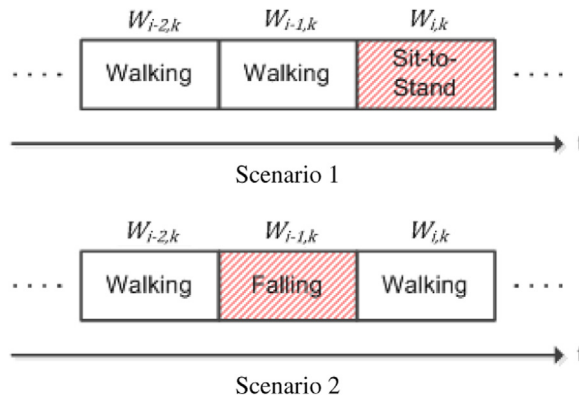


Fig. 9. Two invalid activity transition scenarios which can be detected by the state validator.

4.2. Transition model of physical activities

The transition model of physical activity in the form of Activity Transition Diagram (ATD) is proposed as illustrated in Fig. 8. All activities are represented as states, and the transitions define conditions under which we consider changes of the states. These conditions are not depicted in the figure and will be explained in the following text. The state transitions reflect the possible transitions between activities. For example, from standing position, a person can perform either walking or sitting. There are two possible scenarios of invalid activity transition which can be detected by the state validator as illustrated in Fig. 9. The shaded windows are misclassified. The first scenario involves the occurrence of invalid activity transition due to misclassification of current window, $W_{i,k}$. As shown in Fig. 9, activity transition from walking activity ($W_{i-1,k}$) to sit-to-stand activity ($W_{i,k}$) is an invalid transition, which will be detected by the state validator. In the second scenario, the current window, $W_{i,k}$ is correctly classified, but violation of activity transition is caused due to misclassification of the previous window, $W_{i-1,k}$. As shown in Fig. 9, walking activity ($W_{i,k}$) is correctly classified but an invalid activity transition is detected (falling to walking) due to misclassification on $W_{i-1,k}$. However no invalid activity transition was detected from previous window because walking to falling is a valid transition. Note that, the state validator can only detect invalid activity transition by checking the activity transition from the previous window to current window. But it does not know which window is being misclassified.

In the case of invalid activity transition, the state validator will notify the classification system to re-perform classification on the windows. The re-classification algorithm is given in Fig. 10. The algorithm begins by calculating features of window $W_{i-1,k}$. Then, using the ATD, all possible next activities of the previous window (i.e. $W_{i-2,k}$) are acquired for reclassifying $W_{i-1,k}$.

Using scenario 2 as an example, the algorithm will acquire next possible activities of window $W_{i-2,k}$ (walking) which are walking, falling, standing and stand-to-sit. Next, for each next possible activity, the probability density functions of extracted features are calculated using the multivariate Gaussian distribution explained in Section 4.1. Among the possible next activities, the one that has the highest probability density function value will now be assigned as the state of window $W_{i-1,k}$. Then, the same process is repeated for window $W_{i,k}$. Notice that, the algorithm performs re-classification on the

$W_{x,k}$ is a window after k expansion being classified where $x = i - 1, i$, with $W_{i,k}$ representing the current window.

A is a list of N possible valid activities, with a_j represents a single activity where $j = 1 \dots N$

p_{max} is the maximum probability density function value for a possible activity to determine the activity (state) of the window.

```

if invalid activity transition is detected then
  for  $x = i - 1$  until  $i$  do
    calculate features of  $W_x$ 
     $A =$  get next possible activities of  $A_{W_{x-1,k}}$ 
    for all  $a_j$  in  $A$  do
       $p_{a_j} =$  calculate probability density function of  $a_j$ 
      if  $p_{a_j} > p_{max}$  then
         $p_{max} = p_{a_j}$ 
         $A_{W_{x,k}} = a_j$ 
      end if
    end for
  end for
end if

```

Fig. 10. Re-classification algorithm.

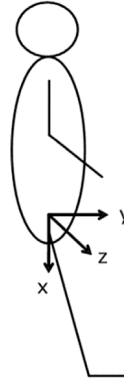


Fig. 11. The sensor position and its coordinate system.

current window and its previous window to handle both invalid transition scenarios without having any prior knowledge on which one is misclassified. In order not to invalidate all previous activity transitions, the algorithm acquires only valid next activities of the previous window to perform re-classification.

5. Experimental setup for physical activity recognition

5.1. Device and data collection

Digital tri-axial accelerometer is a sensing device which can measure the acceleration in three mutually orthogonal directions. Virtenio Preon32 wireless sensor node with a digital tri-axial accelerometer is used in this research for data acquisition. The accelerometer is configured to collect acceleration in the range of ± 4.0 g at a sampling rate of 50 Hz during the experiments. Previous study results show that sampling rate beyond 20 Hz increases recognition accuracy by just 1% and without further improvements beyond 50 Hz [57]. Therefore, sampling rate of 50 Hz is considered to be sufficient. A single tri-axial accelerometer worn on the right waist achieved the highest recognition accuracy in a single sensor comparison study [39,57,58] and hence is used in this research. The sensor position with its coordinate system is illustrated in Fig. 11.

The accelerometer measures acceleration along X-axis or vertical axis (A_x), Y-axis or horizontal axis (A_y) and Z-axis or sideway axis (A_z). The low pass filter with 0.5 Hz cutoff frequency f_c is applied to separate the acceleration force from gravity force. The separation process produces linear acceleration (LA_i) and is performed for each axis to generate LA_x , LA_y , and LA_z . Acceleration and linear acceleration in the horizontal plane (A_{yz} and LA_{yz}), vertical plane (A_{xy} and LA_{xy}) and resultant acceleration (A_{xyz} and LA_{xyz}) are derived from raw and linear acceleration. The tilt angle (TA) of the body trunk can be derived by $\cos^{-1} LA_x/LA_{xyz}$. In total, thirteen signals including the raw acceleration, linear acceleration, horizontal and vertical plane acceleration, resultant acceleration and tilt angle are investigated. Table 2 list all the thirteen signals.

Table 2
Summary of the thirteen signals.

Signals	Descriptions
A_x	Vertical axis (X-axis)
A_y	Horizontal axis (Y-axis)
A_z	Sideway axis (Z-axis)
A_{xy}	Vertical plane
A_{yz}	Horizontal plane
A_{xyz}	Resultant acceleration
LA_x	Linear acceleration of vertical axis
LA_y	Linear acceleration of horizontal axis
LA_z	Linear acceleration of sideway axis
LA_{xy}	Linear acceleration of vertical plane
LA_{yz}	Linear acceleration of horizontal plane
LA_{xyz}	Linear acceleration of resultant acceleration
TA	Tilt angle of the body trunk

Table 3
Categories of physical activities.

Dynamic	Static	Transitional
Walking	Standing	Stand-to-sit
	Sitting	Sit-to-stand
	Lying face-up	Sit-to-lie
	Lying face-down	Lie-to-sit
		Falling

Six healthy volunteers (4 males, age: 33 ± 2.2 years, 1 female, age: 33 years), and a kid (female, age: 10 years) were asked to wear the tri-axial accelerometer on their right waist. Each subject was asked to perform the activities described in Table 3 in their own preferred style and pace. No specific instructions were given about how to perform the activities. All activities were performed continuously for a single trial in a house which consisted of a corridor, a lounge and a bedroom. The length of the corridor and the distance from a room to another is about 10–15 m. Each volunteer was asked to conduct each experiment five times in their own pace.

5.2. Pre-processing and feature selection

Moving average filter is applied to remove high frequency noise. As shown in Table 4, thirteen features are extracted for activity recognition. The slope of signal is calculated by using linear regression technique, which fits a straight line through the signal. Mean Trend and Windowed Mean Difference introduced by [55] describes the trend of mean values over the window. The window is divided into N sub-windows with no overlap. Then the mean of each sub-window, μ_i is calculated. Mean Trend and Windowed Mean Difference are computed as follows.

$$|\mu T| = \sum_{i=2}^N |\mu_i - \mu_{i-1}| \quad (4)$$

$$|\mu D| = \sum_{i=1}^N |\mu - \mu_i|. \quad (5)$$

In this study, we have investigated the variants of the features by not taking the absolute difference in order to obtain the trend (increasing or decreasing) of signal as follows.

$$\mu T, \mu D = \begin{cases} > 0 \text{ trend of signal is increasing} \\ < 0 \text{ trend of signal is decreasing.} \end{cases} \quad (6)$$

All thirteen features are extracted from each of the thirteen signals. Therefore, a total of 169 features are extracted from the acceleration, linear acceleration and tilt angle signals. Waikato Environment for Knowledge Analysis (WEKA) toolkit is used to analyze the features [59].

Features are extracted from the acceleration and linear acceleration data over the sliding window. Najafi et al. investigated the correlation of temporal postural duration with falling risk in elderly people [11], and it is found that the average of postural duration is 2.95 s. Therefore, the initial window size is set to 3 s (150 samples). We have chosen overlapping factor (*of*) of 0.5 and expansion factor (*ef*) of 0.5. The three classifiers are implemented as Decision Tree. Decision Tree is chosen in this study due to its short execution and training time [57]. Furthermore, Decision Tree is found to give the highest levels of classification accuracy according to [15]. ID3 algorithm is used to construct the Decision Tree classifiers [60]. The algorithm determines the threshold value that gives the best separation of samples to effectively distinguish between

Table 4
Initial set of features for activity recognition.

Feature	Key
Average	Avg
Standard deviation	Std
Skewness	SK
Signal magnitude area	SMA
Slope	M
Absolute slope	AM
Spectral energy	E
Mean trend	$ \mu T , \mu T$
Windowed mean difference	$ \mu D , \mu D$
Maximum	Max
Minimum	Min

Table 5
Features of the decision tree classifier for UoA and SBHAR datasets.

	UoA	SBHAR
Transitional activity detector	AM A_y	$ \mu D A_y$
Non-transitional activity classifier	Avg LA_{yz} , Avg A_y	Avg LA_{xy} , Avg A_y
Transitional activity classifier	$\mu T A_y$, Avg A_y	M A_y , Avg A_y

classes, in this case activities. This is achieved by finding the value of threshold that maximizes the information gain. The implementation of the classifiers are described as follows.

For the Transitional Activity Detector, the signals (acceleration and linear acceleration) are segmented by the fixed initial window size and divided into non-transitional activity and transitional activity signals. The thirteen features are calculated using the segmented signals, and Relief-F is used to select the most relevant features against target activities. Relief-F is chosen because of its speed and simplicity [61]. Then, ID3 algorithm is used to construct the Decision Tree classifier.

For training the Non-transitional (Dynamic/Static) Activity Classifier, all non-transitional activity signals are segmented and divided into walking, standing, sitting, lying face-up and lying face-down classes. The thirteen features are calculated using the fixed 3 s signal segments, and Relief-F is used to select the most relevant features against target activities. ID3 algorithm is used to construct the Decision Tree classifier.

For the Transitional Activity Classifier, all transitional activity signals are segmented and divided into stand-to-sit, sit-to-stand, sit-to-lie, lie-to-sit and falling. Transitional activity signals are of different durations. Therefore, the size of the window to calculate the features are varies from one signal to another. The algorithm expands the window by expansion factor, ef which is 1.5 s (75 samples). Hence, the window size to calculate the features are 3 s (150 samples), 4.5 s (225 samples), 6 s (300 samples) etc. depending on the length of the signals. Relief-F is used to select the most relevant features against target activities. Then ID3 algorithm is used to construct the Decision Tree classifier. The features of each classifier for both datasets are given in Table 5. Notice that the selected features may be different due to varying sensor location and types of activities.

During window expansion process, multivariate Gaussian distribution is used to determine the most effective window expansion based on the probability density function. Furthermore, multivariate Gaussian distribution is also used to re-perform classification if invalid activity transition is detected by the ATD. Two features from decision tree classifier (Avg LA_{yz} and Avg A_y) are used to model the distribution. $\mu T A_y$ is not effective to capture the trend of the activity signal when determining the most effective window expansion. An example of this scenario is shown in Fig. 12. As can be seen in Fig. 12, $\mu T A_y$ values of $W_{i,1}$ (−7.579) and $W_{i,2}$ (−7.574) are almost the same, and the PDF value is increasing due to the flat trend of the signal. As a result, the window continues expanding and the most effective window segmentation cannot be identified. Therefore, M A_y is selected to model the distribution since it has the highest information gain after $\mu T A_y$ during feature selection process. Fig. 13 shows how the slope of fitted lines can effectively capture the trend of an activity signal. Three lines, M1, M2 and M3 are fitted through the activity signal for each window expansion. As can be seen, the slope of the fitted line is decreasing as more samples (of other activity signal) are segmented by the window and as a result the PDF value is decreasing.

5.3. Physical activity recognition

We have applied the proposed algorithm to develop a physical activity recognition system. The system is implemented in MATLAB. The specification of the computer used was as follows: Intel Core i7 CPU 2.50 GHz, 12.0 GB RAM, Windows 7. The average durations of data are 90 s and 337 s for UoA and SBHAR respectively. The average of running times are 260.26 and 894.73 ms. An internal (UoA) and public (SBHAR) [54] datasets are used to evaluate the proposed algorithm. SBHAR dataset contains activity signals collected gathered from a smartphone inertial sensors (accelerometer and gyroscope). 30 subjects were asked to perform six basic activities. The position of the device is different to our experiment where

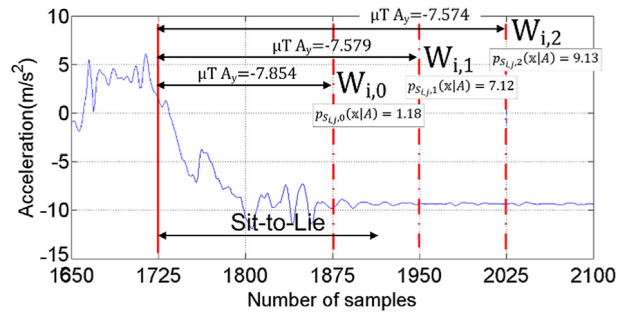


Fig. 12. The values of $\mu T A_y$ for each window expansion.

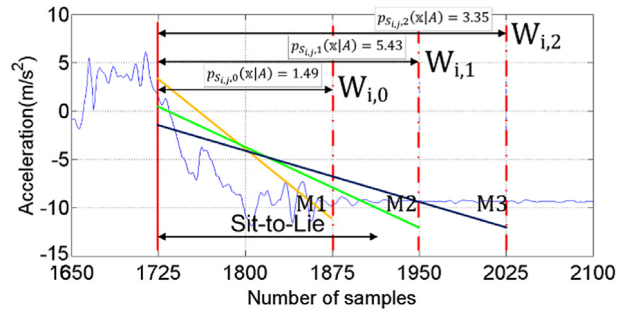


Fig. 13. Fitted lines through acceleration Y signal for each window expansion.

Table 6

Average \pm standard deviation duration and maximum duration of UoA and SBHAR datasets transitional activities.

Transitional activity	UoA		SBHAR	
	Average \pm standard deviation duration (s)	Maximum duration	Average \pm standard deviation duration (s)	Maximum duration
Stand-to-sit	2.96 \pm 0.61	4.60	3.41 \pm 0.8	4.50
Sit-to-stand	2.34 \pm 0.43	3.30	2.57 \pm 0.5	3.70
Sit-to-lie	3.22 \pm 0.76	5.30	4.12 \pm 0.8	7.10
Lie-to-sit	3.01 \pm 0.69	5.20	3.69 \pm 0.7	7.30
Stand-to-lie	N.A.	N.A.	4.95 \pm 1.4	8.40
Lie-to-stand	N.A.	N.A.	3.72 \pm 0.8	11.20
Falling	2.99 \pm 0.64	4.30	N.A.	N.A.

it was attached to the front waist instead of right waist. The dataset includes six transitional activities: stand-to-sit, sit-to-stand, sit-to-lie, lie-to-sit, stand-to-lie and lie-to-stand. Stand-to-lie is actually a sequence of other two transitional activities (stand-to-sit and sit-to-lie). Similarly, lie-to-stand is actually a sequence of lie-to-sit and sit-to-stand activities. The labels were defined between the end and the start of consecutive static activities. The experiments generated 5 h of data. Table 6 shows the average, standard deviation and maximum durations of the transitional activities for both datasets. We randomly chose 10 out of 30 data to train the model for both datasets. Then, the model was tested on the 30 data. Only accelerometer signals are considered for the purpose of this research. Gupta and Dallas (later referred to as GD approach) [55] have introduced new features to effectively recognize transitional activities. The features are mean trend, windowed mean difference, variance trend, windowed variance difference, detrended fluctuation analysis coefficient, energy uncorrelated and maximum difference acceleration. Naïve Bayes and k-NN are used to recognize the activities with a fixed window size of 6 s. We implemented the GD approach using the Naïve Bayes classifier since it achieved better accuracy when classifying transitional activities. We have compared their approach with the proposed adaptive sliding window approach in terms of recognition accuracy. We also investigated the effectiveness of the integration of ATD in the classification algorithm. Comparison with fixed sliding window approach is described in [62]. In comparison with [62], the multivariate Gaussian distribution, rather than Gaussian naïve Bayes, is used to model the transitional activity signals, which allows the correlation of multiple features and their relevance to be modeled. Furthermore, activity transition diagram is introduced to validate the activity transition. As a result, the classification accuracy is improved.

Table 7
Comparison of accuracy of activity recognition.

	Recall (transitional)	Recall (non-transitional)	Overall recall
GD approach	88.7%	90.5%	89.9%
AW approach	93.6%	92.9%	93.0%
AW-TD approach	95.3%	95.4%	95.4%

Table 8
Confusion matrix of GD approach.

	Walk	St-Si	Si-St	Si-Li	Li-Si	Fall	Stand	Sit	Li-up	Li-dw	Count	Recall
Walk	183	10	3	0	0	3	0	0	0	0	199	92.0%
St-Si	3	67	0	11	0	0	0	0	0	0	81	82.7%
Si-St	8	0	69	0	3	1	0	0	0	0	81	85.2%
Si-Li	0	0	0	41	1	0	0	0	0	0	42	97.6%
Li-Si	0	0	1	0	30	0	0	0	0	0	31	96.8%
Fall	1	0	0	0	0	52	0	0	0	4	57	91.2%
Stand	7	0	2	0	0	0	50	0	0	0	59	84.7%
Sit	0	6	5	1	0	0	3	73	0	0	88	83.0%
Li-up	0	0	0	6	2	0	0	3	83	0	94	88.3%
Li-dw	0	0	0	0	0	0	0	0	0	98	98	100%

Table 9
Confusion matrix of AW approach.

	Walk	St-Si	Si-St	Si-Li	Li-Si	Fall	Stand	Sit	Li-up	Li-dw	Count	Recall
Walk	446	21	39	0	0	0	4	0	0	0	510	87.5%
St-Si	0	84	1	1	0	2	0	0	0	0	88	95.5%
Si-St	2	1	83	0	2	0	0	0	0	0	88	94.3%
Si-Li	0	0	0	56	0	0	0	0	3	0	59	94.9%
Li-Si	0	0	0	0	37	0	0	0	2	0	39	94.9%
Fall	4	0	4	0	0	62	0	0	0	0	70	88.6%
Stand	3	1	0	0	0	0	138	0	0	0	142	97.2%
Sit	2	1	2	0	0	0	6	215	0	0	226	95.1%
Li-up	0	0	0	12	0	0	0	0	223	0	235	94.9%
Li-dw	3	0	0	0	0	1	0	0	0	212	216	98.1%

6. Results and discussion

6.1. UoA: the University of Auckland dataset

We compute and tabulate the accuracy of the recognition from the values of true positive (TP), false positive (FP) and false negative (FN) to evaluate the performance of the proposed approach. Recall or true positive rate is the number of windows that are correctly classified and is given by

$$\text{Recall} = TP / (TP + FN) . \quad (7)$$

In addition to the recall, we calculated the precision and F-score metrics [49]. The additional metrics are given in Fig. 15.

Table 7 compares the recall measures of activity recognition system using adaptive sliding window approach with (AW-TD) and without (AW) ATD against the existing GD approach. Tables 8–10 show the performance of the approaches by means of confusion matrices. The recognition accuracy of individual activities, transitional activities, non-transitional activities and the overall accuracy are compared and analyzed. In general, GD approach performed reasonably well in classifying most activities and achieved an overall accuracy of 89.9%, which is 5.5% lower than the proposed AW-TD approach. For the AW-TD approach, classification accuracy is over 90% for every individual activity. For AW approach, although the overall accuracy is only marginally lower (2.4% less) compared with AW-TD, the standard deviation in classification accuracy is higher, which are 3.4% for AW and 2.1% for AW-TD. This indicates AW approach is less accurate in some activities while AW-TD provides good classification in every case.

As for classifying transitional activities, GD approach achieved 88.7% accuracy. Majority of the transitional activities can be classified with 91.2%–97.6% accuracy range with the exception of stand-to-sit which was poorly classified with only 82.7% accuracy. This reflects the fact that GD approach cannot handle activity signal with varying length as shown in Fig. 14. The length of stand-to-sit signal in Fig. 14(a) is about 2 s (100 samples) while stand-to-sit signal in Fig. 14(b) is about 3.5 s (175 samples). As can be seen in Fig. 14(a), walking signal occupies almost half of the window, which leads to misclassification. Conversely, AW-TD approach achieved recognition accuracy of 95.3% in transitional activities. It successfully detected the activities and adapted the window size to accommodate activity signals of varying lengths. However, GD approach achieved slightly higher accuracy, about 1.9% and 2.7%, in classifying Lie-to-Sit and Sit-to-Lie respectively than AW-TD approach. This is because, in the experiments, AW-TD approach failed to detect transitional activity signal at the beginning and hence

Table 10
Confusion matrix of AW-TD approach.

	Walk	St-Si	Si-St	Si-Li	Li-Si	Fall	Stand	Sit	Li-up	Li-dw	Count	Recall
Walk	484	10	11	0	0	1	4	0	0	0	510	94.9%
St-Si	0	87	0	1	0	0	0	0	0	0	88	98.9%
Si-St	2	1	84	1	0	0	0	0	0	0	88	95.5%
Si-Li	0	0	0	56	0	0	0	0	3	0	59	94.9%
Li-Si	0	0	0	0	37	0	0	0	2	0	39	94.9%
Fall	4	2	0	0	0	64	0	0	0	0	70	91.4%
Stand	2	3	0	0	0	0	137	0	0	0	142	96.5%
Sit	0	2	8	0	0	0	4	212	0	0	226	93.8%
Li-up	0	0	0	12	0	0	0	0	223	0	235	94.9%
Li-dw	0	0	2	0	0	2	0	0	0	212	216	98.1%

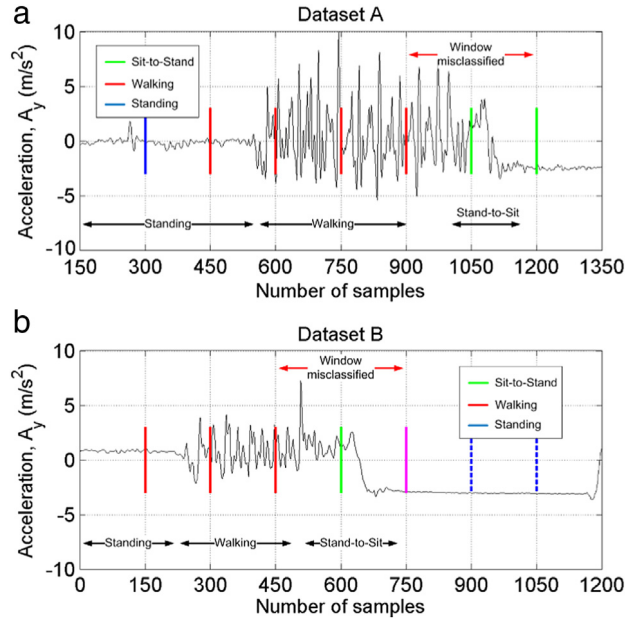


Fig. 14. Stand-to-sit signals with varying length.

adaptive sliding window is not applied. As a result, the window being processed is wrongly classified. It is also observed that in a few experiments, the algorithm failed to determine the best window segmentation due to the over-expansion of the window, which leads to misclassification of the activity. Out of 210 window expansion operations (adaptive window mode), only in 9 cases the windows are not correctly expanded. In total, 4.7% of transitional activity windows were misclassified by AW-TD approach while GD approach misclassified 11.3% of transitional activity windows. This demonstrates that adaptive sliding window segmentation is significantly more effective in classifying transitional activities.

Based on our previous observation, activities are very often misclassified during state transitions due to ambiguous signal characteristics caused by some minor motion behavior change. These can be clearly observed in dynamic behaviors such as walking and falling, as well as standing which is the preceding activity of walking. In AW approach, these activities (walking, falling and standing) are classified relatively poor with only an average of 91.1% accuracy. There is an additional improvement to the overall recognition accuracy when the state validator is integrated into the activity recognition system and acts as a feedback. The recognition accuracy of walking has seen significant improvement whereby more than half of the misclassifications have been corrected. From the observation, the state validator successfully detected the invalid transition when a window is misclassified and the window classification is corrected by the classification system. The overall recognition accuracy is also improved with lower standard deviation, in which recognition accuracy for all activities are well above 90%. However, recognition accuracy of sitting and standing has been decreased by 1.3% and 0.7% respectively. This is because the windows were incorrectly re-classified by multivariate Gaussian distribution.

6.2. SBHAR: smartphone-based HAR dataset

Table 11 compares the recall measures of activity recognition system using GD, AW-TD and AW on the dataset. The recognition accuracy of individual activities, transitional activities, non-transitional activities and the overall accuracy are compared and analyzed. GD approach performed reasonably well in classifying the activities and achieved overall

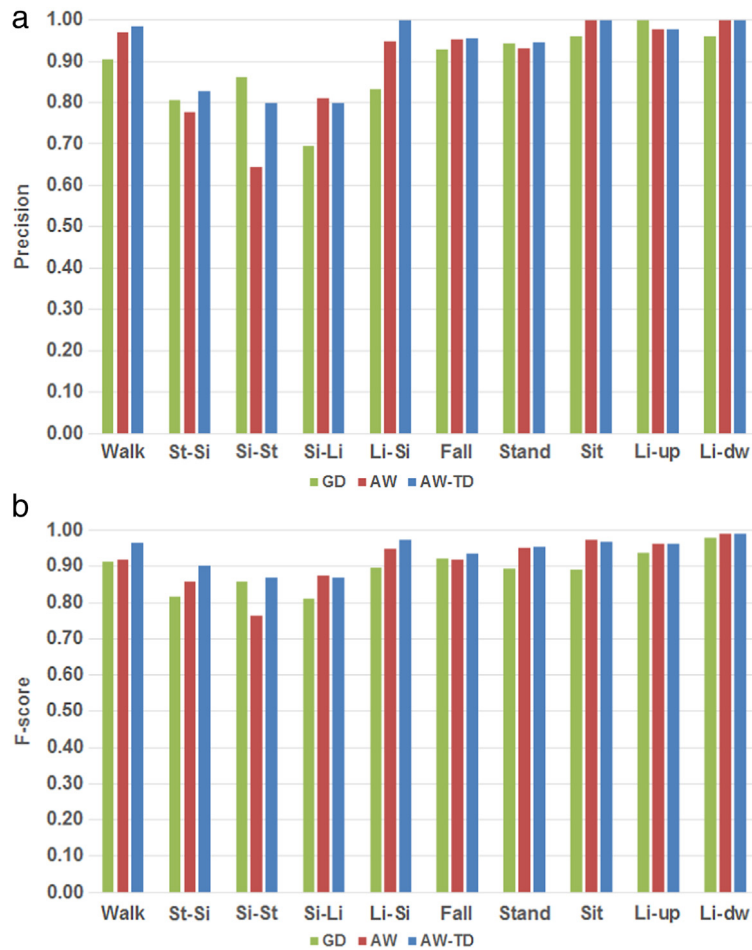


Fig. 15. Comparison of (a) Precision and (b) F-score between GD, AW and AW-TD for UoA dataset.

Table 11
Comparison of accuracy of activity recognition.

	Recall (transitional)	Recall (non-transitional)	Overall recall
GD approach	88.2%	92.4%	91.9%
AW approach	90.3%	96.1%	95.7%
AW-TD approach	95.1%	96.6%	96.5%

accuracy of 91.9% which is 4.6% lower than AW-TD. For AW-TD approach, the classification accuracies for all activities are above 90%, achieving overall recognition accuracy of 96.5% while AW approach achieved an overall recognition accuracy of 95.7%. As for transitional activities, AW-TD performed better in classifying all transitional activities than GD approach, achieving recognition accuracy of 95.1% which is 6.9% higher than GD. The overall recognition accuracy is improved when state validator is integrated into the activity recognition system. Transitional activities have seen significant improvement whereby the accuracy is increased by 4.8%. Tables 12–14 are the confusion matrices of GD, AW and AW-TD approaches. Fig. 16 shows the comparison of precision and F-score between GD, AW and AW-TD.

7. Conclusions

In this paper, we propose a novel adaptive sliding window technique for segmentation of activity signal acquired from tri-axial accelerometer to overcome the limitations of fixed-size sliding window used in existing works. In the proposed approach the window size is adaptively adjusted based on signal information to achieve the more effective window segmentation compared to fixed-size window approaches. In addition, we also proposed a transition model of physical activity to improve classification accuracy. In this study, we demonstrated the performance of the approach on two datasets in which one of them is a public dataset. The employed datasets were generated by different subjects with different styles and pace. It was observed that the system can classify different activities performed by different subjects with excellent accuracy.

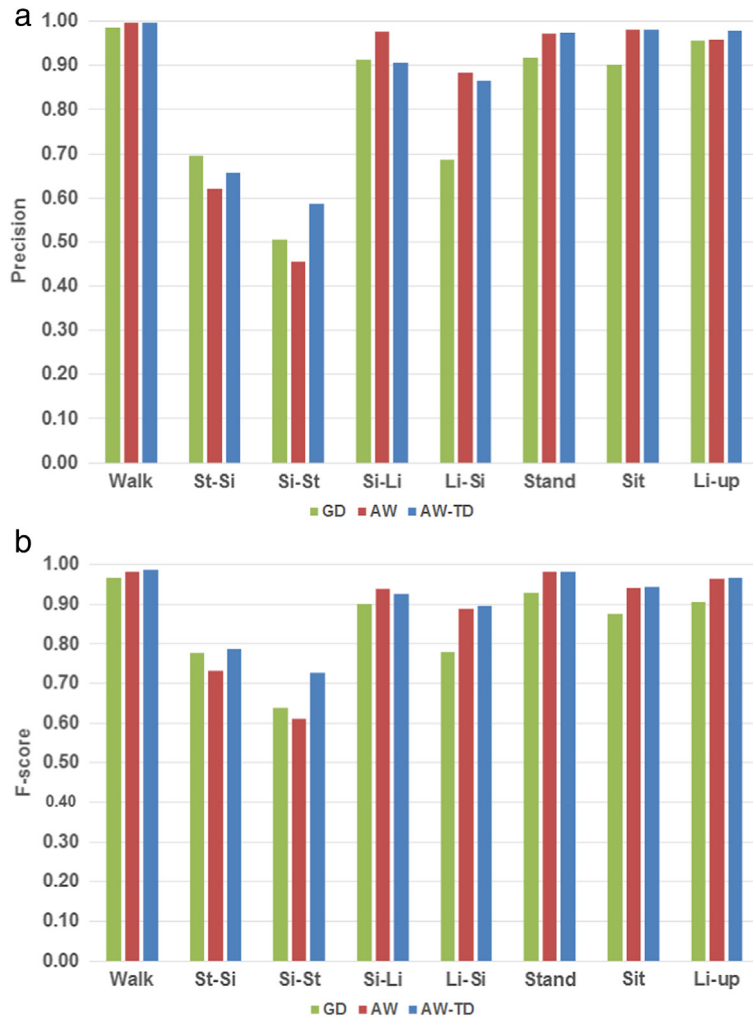


Fig. 16. Comparison of (a) precision and (b) F-score between GD, AW and AW-TD for SBHAR dataset.

Table 12

Confusion matrix of GD approach.

	Walk	St-Si	Si-St	Si-Li	Li-Si	Stand	Sit	Lie	Count	Recall
Walk	1718	19	58	0	1	15	1	0	1812	94.8%
St-Si	5	87	1	6	0	0	0	0	99	87.9%
Si-St	1	2	80	0	10	0	0	0	93	86.0%
Si-Li	0	8	0	94	2	0	0	2	106	88.7%
Li-Si	1	0	7	0	90	0	0	2	100	90.0%
Stand	12	0	8	0	0	362	3	0	385	94.0%
Sit	5	7	2	3	8	11	276	12	324	85.2%
Lie	0	2	2	0	20	7	26	351	408	86.0%

Table 13

Confusion matrix of AW approach.

	Walk	St-Si	Si-St	Si-Li	Li-Si	Stand	Sit	Lie	Count	Recall
Walk	3341	48	68	0	0	1	11	0	3469	96.3%
St-Si	0	116	13	0	0	1	0	0	130	89.2%
Si-St	3	1	92	0	3	0	0	0	99	92.9%
Si-Li	0	10	2	120	0	0	0	1	133	90.2%
Li-Si	0	2	9	0	99	0	0	1	111	89.2%
Stand	2	1	4	0	0	1004	1	0	1012	99.2%
Sit	1	6	9	2	5	12	684	36	755	90.6%
Lie	1	3	5	1	5	16	1	897	929	96.6%

Table 14
Confusion matrix of AW-TD approach.

	Walk	St-Si	Si-St	Si-Li	Li-Si	Stand	Sit	Lie	Count	Recall
Walk	3387	40	41	0	0	1	0	0	3469	97.6%
St-Si	1	127	0	1	0	1	0	0	130	97.7%
Si-St	1	1	94	0	3	0	0	0	99	94.9%
Si-Li	0	4	2	126	0	0	0	1	133	94.7%
Li-Si	0	2	5	0	103	0	1	0	111	92.8%
Stand	4	3	3	0	0	1000	2	0	1012	98.8%
Sit	3	12	11	8	8	9	685	19	755	90.7%
Lie	1	4	4	4	5	16	10	885	929	95.3%

The results showed that the proposed approach effectively segments activity signals resulting in better classification accuracy in a wide range of activities. The approach specifies small initial window size, which is able to segment dynamic and static activity signals, and expand window size dynamically to accommodate transitional activity signal which is longer than the current window size. The approach determines the optimum window size automatically as the signal is being evaluated. As a result, the window contains the right information when performing classification. Moreover, the state validator, which provides a feedback to the classification system, for activity recognition system is proposed. The state validator performs validation of activity transition for every window classification based on the proposed activity transition model and notifies the classification system to re-perform classification in the case an invalid transition is detected. The results showed that AW-TD achieved 95.4% overall accuracy, which is 2.4% better than AW and 5.5% better than existing GD approach. AW-TD achieved an overall accuracy of 96.5%, which is 0.8% better than AW and 4.6% better than GD when tested on SBHAR dataset. The proposed algorithm could only expand the window size. We plan to explore effects of additional mechanism in which the size of the window could be also reduced dynamically to capture short activity signals and further improve classification accuracy. In future work we plan to analyze the applicability of the algorithm for use in real-time scenarios. This will include the detailed analysis of computational complexity and their effect on real-time properties of the algorithm.

Acknowledgments

The authors would like to thank Embedded System Research Group for providing sensors and devices utilized in this study. The authors would also like to thank Nazrin Muhammad (UoA) for testing of these devices and assisting with this work.

References

- [1] WHO *j* Ageing and life-course, WHO. [Online]. Available: <http://www.who.int/ageing/en/> (Accessed 20 November 2014).
- [2] Ageing characterises the demographic perspectives of the European societies - Issue number 72/2008 - Product - Eurostat. [Online]. Available: <http://ec.europa.eu/eurostat/en/web/products-statistics-in-focus/-/KS-SF-08-072> (Accessed 10 February 2016).
- [3] Q. Ni, A.B. García Hernando, I.P. de la Cruz, The elderly's independent living in smart homes: a characterization of activities and sensing infrastructure survey to facilitate services development, *Sensors* 15 (5) (2015) 11312–11362.
- [4] T. Kleinberger, M. Becker, E. Ras, A. Holzinger, P. Müller, Ambient intelligence in assisted living: enable elderly people to handle future interfaces, in: C. Stephanidis (Ed.), *Universal Access in Human-Computer Interaction. Ambient Interaction*, Springer, Berlin, Heidelberg, 2007, pp. 103–112.
- [5] C. Perera, A. Zaslavsky, P. Christen, D. Georgakopoulos, Context aware computing for the internet of things: A survey, *IEEE Commun. Surv. Tutor.* 16 (1) (2014) 414–454. First.
- [6] H. Viswanathan, B. Chen, D. Pompili, Research challenges in computation, communication, and context awareness for ubiquitous healthcare, *IEEE Commun. Mag.* 50 (5) (2012) 92–99.
- [7] M.M. Gross, P.J. Stevenson, S.L. Charette, G. Pyka, R. Marcus, Effect of muscle strength and movement speed on the biomechanics of rising from a chair in healthy elderly and young women, *Gait Posture* 8 (3) (1998) 175–185.
- [8] B. Unver, V. Karatosun, S. Bakirhan, Ability to rise independently from a chair during 6-month follow-up after unilateral and bilateral total knee replacement, *J. Rehabil. Med.* 37 (6) (2005) 385–387.
- [9] O. Eriksrud, R.W. Bohannon, Relationship of knee extension force to independence in sit-to-stand performance in patients receiving acute rehabilitation, *Phys. Ther.* 83 (6) (2003) 544–551.
- [10] S. Deandrea, F. Bravi, F. Turati, E. Lucenteforte, C. La Vecchia, E. Negri, Risk factors for falls in older people in nursing homes and hospitals. A systematic review and meta-analysis, *Arch. Gerontol. Geriatr.* 56 (3) (2013) 407–415.
- [11] B. Najafi, K. Aminian, F. Loew, Y. Blanc, P.A. Robert, Measurement of stand-sit and sit-stand transitions using a miniature gyroscope and its application in fall risk evaluation in the elderly, *IEEE Trans. Biomed. Eng.* 49 (8) (2002) 843–851.
- [12] L. Nyberg, Y. Gustafson, Patient falls in stroke rehabilitation. A challenge to rehabilitation strategies, *Stroke J. Cereb. Circ.* 26 (5) (1995) 838–842.
- [13] K. Rapp, C. Becker, I.D. Cameron, H.-H. Knig, G. Büchele, Epidemiology of falls in residential aged care: analysis of more than 70,000 falls from residents of bavarian nursing homes, *J. Am. Med. Dir. Assoc.* 13 (2) (2012) 187.e1–187.e6.
- [14] A. Zijlstra, M. Mancini, U. Lindemann, L. Chiari, W. Zijlstra, Sit-stand and stand-sit transitions in older adults and patients with Parkinson's disease: event detection based on motion sensors versus force plates, *J. Neuroeng. Rehabil.* 9 (2012) 75.
- [15] S.J. Preece, J.Y. Goulermas, L.P.J. Kenney, D. Howard, K. Meijer, R. Crompton, Activity identification using body-mounted sensors—a review of classification techniques, *Physiol. Meas.* 30 (4) (2009) R1.
- [16] S. Bersch, D. Azzi, R. Khusainov, I. Achumba, J. Ries, Sensor data acquisition and processing parameters for human activity classification, *Sensors* 14 (3) (2014) 4239–4270.
- [17] O. Banos, J.-M. Galvez, M. Damas, H. Pomares, I. Rojas, Window size impact in human activity recognition, *Sensors* 14 (4) (2014) 6474–6499.
- [18] B. Fida, I. Bernabucci, D. Bibbo, S. Conforto, M. Schmid, Varying behavior of different window sizes on the classification of static and dynamic physical activities from a single accelerometer, *Med. Eng. Phys.* 37 (7) (2015) 705–711.
- [19] D. Weinland, R. Ronfard, E. Boyer, A survey of vision-based methods for action representation, segmentation and recognition, *Comput. Vis. Image Underst.* 115 (2) (2011) 224–241.

- [20] O. Banos, J.-M. Galvez, M. Damas, A. Guillen, L.-J. Herrera, H. Pomares, I. Rojas, Evaluating the effects of signal segmentation on activity recognition, in: Presented at the 2nd International Work-Conference on Bioinformatics and Biomedical Engineering, 2014.
- [21] L. Santos, K. Khoshhal, J. Dias, Trajectory-based human action segmentation, *Pattern Recognit.* 48 (2) (2015) 568–579.
- [22] S. Kozina, M. Lustrek, M. Gams, Dynamic signal segmentation for activity recognition, in: Proceedings of International Joint Conference on Artificial Intelligence, Barcelona, Spain, Vol. 1622, 2011, p. 1522.
- [23] A. Bifet, R. Gavaldà, Learning from time-changing data with adaptive windowing., in *SDM*, Vol. 7, 2007, p. 2007.
- [24] M. Núñez, R. Fidalgo, R. Morales, Learning in environments with unknown dynamics: Towards more robust concept learners, *J. Mach. Learn. Res.* 8 (2007) 2595–2628.
- [25] Z. Sheng, C. Hailong, J. Chuan, Z. Shaojun, An adaptive time window method for human activity recognition, in 2015 IEEE 28th Canadian Conference on Electrical and Computer Engineering, CCECE, 2015, pp. 1188–1192.
- [26] M. Sekine, T. Tamura, T. Togawa, Y. Fukui, Classification of waist-acceleration signals in a continuous walking record, *Med. Eng. Phys.* 22 (4) (2000) 285–291.
- [27] M.N. Nyan, F.E.H. Tay, K.H.W. Seah, Y.Y. Sitoh, Classification of gait patterns in the time–frequency domain, *J. Biomech.* 39 (14) (2006) 2647–2656.
- [28] M. Yoshizawa, W. Takasaki, R. Ohmura, Parameter exploration for response time reduction in accelerometer-based activity recognition, in: Proceedings of the 2013 ACM Conference on Pervasive and Ubiquitous Computing Adjunct Publication, New York, NY, USA, 2013, pp. 653–664.
- [29] D.K. Aminian, K. Rezakhanlou, E.D. Andres, C. Fritsch, P.-F. Leyvraz, P. Robert, Temporal feature estimation during walking using miniature accelerometers: an analysis of gait improvement after hip arthroplasty, *Med. Biol. Eng. Comput.* 37 (6) (1999) 686–691.
- [30] R.W. Selles, M.A.G. Formanoy, J. Bussmann, P.J. Janssens, H.J. Stam, Automated estimation of initial and terminal contact timing using accelerometers; development and validation in transtibial amputees and controls, *IEEE Trans. Neural Syst. Rehabil. Eng.* 13 (1) (2005) 81–88.
- [31] K. Aminian, B. Najafi, C. Büla, P.-F. Leyvraz, P. Robert, Spatio-temporal parameters of gait measured by an ambulatory system using miniature gyroscopes, *J. Biomech.* 35 (5) (2002) 689–699.
- [32] J.M. Jasiewicz, J.H.J. Allum, J.W. Middleton, A. Barriskill, P. Condie, B. Purcell, R.C.T. Li, Gait event detection using linear accelerometers or angular velocity transducers in able-bodied and spinal-cord injured individuals, *Gait Posture* 24 (4) (2006) 502–509.
- [33] M. Benocci, M. Bächlin, E. Farella, D. Roggen, L. Benini, G. Tröster, Wearable assistant for load monitoring: recognition of on-body load placement from gait alterations, in: Pervasive Computing Technologies for Healthcare (PervasiveHealth), 2010 4th International Conference on-NO PERMISSIONS, 2010, pp. 1–8.
- [34] A. Sant’Anna, N. Wickström, A symbol-based approach to gait analysis from acceleration signals: Identification and detection of gait events and a new measure of gait symmetry, *IEEE Trans. Inf. Technol. Biomed.* 14 (5) (2010) 1180–1187.
- [35] L. Chen, J. Hoey, C.D. Nugent, D.J. Cook, Z. Yu, Sensor-based activity recognition, *IEEE Trans. Syst. Man Cybern. Part C Appl. Rev.* 42 (6) (2012) 790–808.
- [36] M. Ermes, J. Parkka, J. Mantyjarvi, I. Korhonen, Detection of daily activities and sports with wearable sensors in controlled and uncontrolled conditions, *IEEE Trans. Inf. Technol. Biomed.* 12 (1) (2008) 20–26.
- [37] A.T. Özdemir, B. Barshan, Detecting falls with wearable sensors using machine learning techniques, *Sensors* 14 (6) (2014) 10691–10708.
- [38] D. De, P. Bharti, S.K. Das, S. Chellappan, Multimodal wearable sensing for fine-grained activity recognition in healthcare, *IEEE Internet Comput.* 19 (5) (2015) 26–35.
- [39] L. Bao, S.S. Intille, Activity recognition from user-annotated acceleration data, in: A. Ferscha, F. Mattern (Eds.), Pervasive Computing, Springer, Berlin, Heidelberg, 2004, pp. 1–17.
- [40] R. Jia, B. Liu, Human daily activity recognition by fusing accelerometer and multi-lead ECG data, in: 2013 IEEE International Conference on Signal Processing, Communication and Computing, ICSPCC, 2013, pp. 1–4.
- [41] J.-H. Chiang, P.-C. Yang, H. Tu, Pattern analysis in daily physical activity data for personal health management, *Pervasive Mob. Comput.* 13 (2014) 13–25.
- [42] P.H.F. Peeters, Design criteria for an automatic safety-alarm system for elderly, *Technol. Health Care* 8 (2) (2000) 81–91.
- [43] R. Adaskevicius, Method for recognition of the physical activity of human being using a wearable accelerometer, *Elektron. Elektrotechn.* 20 (5) (2014) 127–131.
- [44] L. Hu, Y. Chen, S. Wang, Z. Chen, b-COELM: A fast, lightweight and accurate activity recognition model for mini-wearable devices, *Pervasive Mob. Comput.* 15 (2014) 200–214.
- [45] C. Catal, S. Tufekci, E. Pirmitt, G. Kocabag, On the use of ensemble of classifiers for accelerometer-based activity recognition, *Appl. Soft Comput.* 37 (2015) 1018–1022.
- [46] W. Xiao, Y. Lu, W. Xiao, Y. Lu, Daily human physical activity recognition based on kernel discriminant analysis and extreme learning machine, *daily human physical activity recognition based on kernel discriminant analysis and extreme learning machine*, *Math. Probl. Eng.* (2015) e790412. 2015.
- [47] Z. He, Activity recognition from accelerometer signals based on Wavelet-AR model, in: 2010 IEEE International Conference on Progress in Informatics and Computing PIC, Vol. 1, 2010, pp. 499–502.
- [48] S.J. Preece, J.Y. Goulermas, L.P.J. Kenney, D. Howard, A comparison of feature extraction methods for the classification of dynamic activities from accelerometer data, *IEEE Trans. Biomed. Eng.* 56 (3) (2009) 871–879.
- [49] O.D. Lara, M.A. Labrador, A survey on human activity recognition using wearable sensors, *IEEE Commun. Surv. Tutor.* 15 (3) (2013) 1192–1209. Third.
- [50] S. Kozina, H. Gjoreski, M. Gams, M. Luštrek, Three-layer activity recognition combining domain knowledge and meta-classification, *J. Med. Biol. Eng.* 33 (4) (2013) 406–414.
- [51] Y. Zhang, S. Markovic, I. Sapir, R.C. Wagenaar, T.D.C. Little, Continuous functional activity monitoring based on wearable tri-axial accelerometer and gyroscope, in: 2011 5th International Conference on Pervasive Computing Technologies for Healthcare (PervasiveHealth), 2011, pp. 370–373.
- [52] V. Ahanathapillai, J.D. Amor, M. Tadeusiak, C.J. James, Wrist-Worn Accelerometer to Detect Postural Transitions and Walking Patterns, in: L.M.R. Romero (Ed.), XIII Mediterranean Conference on Medical and Biological Engineering and Computing 2013, Springer International Publishing, 2014, pp. 1515–1518.
- [53] A. Khan, Y.-K. Lee, S.Y. Lee, T.-S. Kim, A triaxial accelerometer-based physical-activity recognition via augmented-signal features and a hierarchical recognizer, *IEEE Trans. Inf. Technol. Biomed.* 14 (5) (2010) 1166–1172.
- [54] J.-L. Reyes-Ortiz, L. Oneto, A. Samà, X. Parra, D. Anguita, Transition-aware human activity recognition using smartphones, *Neurocomputing* 171 (2016) 754–767.
- [55] P. Gupta, T. Dallas, Feature selection and activity recognition system using a single triaxial accelerometer, *IEEE Trans. Biomed. Eng.* 61 (6) (2014) 1780–1786.
- [56] A.C. Rencher, W.F. Christensen, *Methods of Multivariate Analysis*, John Wiley & Sons, 2012.
- [57] L. Gao, A.K. Bourke, J. Nelson, Evaluation of accelerometer based multi-sensor versus single-sensor activity recognition systems, *Med. Eng. Phys.* 36 (6) (2014) 779–785.
- [58] S.G. Trost, Y. Zheng, W.-K. Wong, Machine learning for activity recognition: hip versus wrist data, *Physiol. Meas.* 35 (11) (2014) 2183.
- [59] Weka 3 - Data Mining with Open Source Machine Learning Software in Java. [Online]. Available: <http://www.cs.waikato.ac.nz/ml/weka/> (Accessed 11 August 2015).
- [60] J.R. Quinlan, Induction of decision trees, *Mach. Learn.* 1 (1) (1986) 81–106.
- [61] L. Atallah, B. Lo, R. King, G.-Z. Yang, Sensor positioning for activity recognition using wearable accelerometers, *IEEE Trans. Biomed. Circuits Syst.* 5 (4) (2011) 320–329.
- [62] M.H.M. Noor, Z. Salcic, K.I.-K. Wang, Dynamic sliding window method for physical activity recognition using a single tri-axial accelerometer, in: 2015 IEEE 10th Conference on Industrial Electronics and Applications, ICIEA, 2015, pp. 102–107.